Published in final edited form as:

ACS Chem Biol. 2016 January 15; 11(1): 200–210. doi:10.1021/acschembio.5b00740.

Transportable, Chemical Genetic Methodology for the Small Molecule-Mediated Inhibition of Heat Shock Factor 1

Christopher L. Moore[1], **Mahender B. Dewal**[1], **Emmanuel E. Nekongo**[1], **Sebasthian Santiago**[1], **Nancy B. Lu**[1], **Stuart S. Levine**[2], and **Matthew D. Shoulders**[1,*]

[1]Department of Chemistry, Massachusetts Institute of Technology, Cambridge, MA 02139

[2]BioMicro Center, Massachusetts Institute of Technology, Cambridge, MA 02139

Abstract

Proteostasis in the cytosol is governed by the heat shock response. The master regulator of the heat shock response, heat shock factor 1 (HSF1), and key chaperones whose levels are HSF1-regulated have emerged as high-profile targets for therapeutic applications ranging from protein misfolding-related disorders to cancer. Nonetheless, a generally applicable methodology to selectively and potently inhibit endogenous HSF1 in a small molecule-dependent manner in disease model systems remains elusive. Also problematic, the administration of even highly selective chaperone inhibitors often has the side effect of activating HSF1 and thereby inducing a compensatory heat shock response. Herein, we report a ligand-regulatable, dominant negative version of HSF1 that addresses these issues. Our approach, which required engineering a new dominant negative HSF1 variant, permits doseable inhibition of endogenous HSF1 with a selective small molecule in cell-based model systems of interest. The methodology allows us to uncouple the pleiotropic effects of chaperone inhibitors and environmental toxins from the concomitantly induced compensatory heat shock response. Integration of our method with techniques to activate HSF1 enables the creation of cell lines in which the cytosolic proteostasis network can be up- or down-regulated by orthogonal small molecules. Selective, small molecule-mediated inhibition of HSF1 has distinctive implications for the proteostasis of both chaperone-dependent globular proteins and aggregation-prone intrinsically disordered proteins. Altogether, this work provides critical methods for continued exploration of the biological roles of HSF1 and the therapeutic potential of heat shock response modulation.

Keywords

HSF1; heat shock response; proteostasis; HSP90 inhibition; arsenite; destabilized domain; chaperone

*To whom correspondence should be addressed: Matthew D. Shoulders, Department of Chemistry, Massachusetts Institute of Technology, 77 Massachusetts Avenue, Building 16, Room 573A, Cambridge, MA 02139, Phone: (617) 452-3525, Fax: (617) 324-0505, ; Email: mshoulde@mit.edu

Supporting Information

The Supporting Information is available free of charge on the ACS Publications website.

Supporting Information Figures S1 and S2 and Supporting Information Tables S1–S3. Complete experimental procedures for qPCR experiments, lentivirus production, and whole genome array analyses (PDF).

INTRODUCTION

The heat shock response (HSR) maintains cytosolic proteostasis by dynamically matching cellular protein folding capacity to demand and environmental conditions.[1] Acute protein folding insults, such as heat or oxidative stress, as well as chronic misfolding and protein aggregation activate the HSR, thereby transcriptionally upregulating chaperones and quality control factors that coordinate to address the proteostatic challenge.[2] Induction of these proteostasis mechanisms is mediated by the master regulator of the HSR, the transcription factor heat shock factor 1 (HSF1).[3] Under unstressed conditions, the majority of cellular HSF1 is maintained in a monomeric state in the cytosol. Protein misfolding insults instigate a shift towards nuclear, trimeric, and transcriptionally active HSF1.[4] Molecular details of the HSF1 activation mechanism remain under investigation, but chaperone binding to maintain HSF1 in its inactive, monomeric form and post-translational modifications play important roles.[5,6]

HSF1 inhibition has recently emerged as a promising therapeutic strategy for a diverse array of cancers.[7] Of particular note, genetic ablation of HSF1 attenuates resistance to tumorigenesis in mice,[8] constitutive upregulation of HSF1 is linked to poor breast cancer patient prognosis,[9] and HSF1 activation in cancer-associated fibroblasts promotes malignancy.[10] Interestingly, HSF1 in malignant cells regulates the expression of numerous genes not typically associated with the HSR,[11] suggesting multiple roles for this master regulator of proteostasis in pathologic processes. These and other findings motivate HSF1 inhibition as a potentially useful anti-cancer therapeutic strategy.[12]

Surprisingly, HSF1 inhibition is also emerging as a possible strategy for diseases linked directly to protein misfolding or aggregation.[13] Balch and co-workers identified a “maladapted stress response” mediated by chronic upregulation of HSF1 in diverse protein misfolding-related disorders, including cystic fibrosis.[14] They found that genetic elimination of HSF1 restored disease-associated proteostasis defects, possibly by reducing hyperactive quality control mechanisms chronically upregulated by HSF1. The counter-intuitive possibility that HSF1 inhibition could be valuable in certain protein misfolding diseases further enhances the appeal of small molecule-based methods to explore the therapeutic potential of HSF1 inhibition.

These and other findings have engendered active efforts to discover inhibitors of HSF1.[7,15] Unfortunately, the identification of potent and selective small molecule-based inhibitors of transcription factors remains a challenging endeavor. Although a number of compounds capable of inhibiting HSF1 have been identified, including triptolide, NZ28, rohitinib, cantharidin, and more,[7,15–18] mechanistic studies show that these compounds have pleiotropic effects at the concentrations required for HSF1 inhibition, and several lack potency.[16,19,20] In the absence of selective and potent small molecule inhibitors of HSF1, researchers have focused on genetic techniques to ablate HSF1 activity, such as RNAi against HSF1 or constitutive over-expression of dominant negative HSF1 variants that can inhibit the endogenously expressed transcription factor.[14,21–26] These approaches have the advantage of high selectivity and potency, but at the cost of slow kinetics, poor dosability,

and cellular adaptation or even death upon chronic HSF1 knockdown or constitutive dominant negative HSF1 overexpression.[27]

An alternative to HSF1 inhibition is targeting the activities of downstream effectors of proteostasis. In this regard, inhibitors of the cytosolic HSP90 and HSP70 chaperones are of substantial interest. Clinical trials testing HSP90 inhibitors in oncology are ongoing, and increasingly potent and selective HSP70 inhibitors continue to be developed.[28,29] Such chaperone inhibitors are ubiquitously deployed in the literature to evaluate effects of chaperone inhibition on client protein folding and function. A sometimes underappreciated complication for mechanistic studies does, however, exist: many chaperone inhibitors activate a compensatory HSR mediated by HSF1.[30] The consequence is that chaperone inhibition can actually induce high levels of other chaperones and quality control mechanisms, potentially engendering the wrongful attribution of observed phenotypes directly to chaperone inhibition rather than to the compensatory HSR. Similarly problematic, the compensatory HSR can obscure consequences of chaperone inhibition.[31] In malignant cells, this issue can sometimes be resolved by very carefully fine-tuning the dose of HSP90 inhibitor to sidestep the compensatory HSR, but the acceptable dose range for an inhibitory effect without HSR induction is narrow and often non-existent. Alternatively, a promising new class of HSP90 inhibitor is emerging that functions by binding to the chaperone's C-terminus and does not activate the HSR.[32,33] These compounds require continued development for potency and selectivity.[34] In summary, methods to uncouple the direct effects of chaperone inhibition from the compensatory HSR would be very valuable, not just for elucidating the mechanistic consequences of chaperone inhibition, but also for studying the roles of the HSR in protection against other HSR activators like the environmental toxin arsenite.[35]

Small molecule-based methods to potently and selectively inhibit HSF1 are, therefore, urgently required. Here, we report the development of new small molecule-regulated, genetically-encoded dominant negative versions of HSF1 that can be easily deployed in diverse model systems of interest. Our approach enables the robust uncoupling of the HSF1-activating side effects of chaperone inhibition or oxidative stress from their direct effects on cellular proteostasis. Importantly, our method is synergistic with and orthogonal to a previously reported approach for small molecule-regulated *activation* of HSF1,[36] allowing us to inducibly activate or repress the cytosolic proteostasis network with small molecules in a single cell, as desired. Finally, we evaluate the implications of small molecule-mediated HSF1 inhibition for the proteostasis of model globular and aggregating cytosolic chaperone clients. Altogether, our work provides a robust methodology valuable for continued studies of the normal and pathologic roles of HSF1 that will inform the continued development of HSF1 regulators for applications in cancer and protein misfolding-related diseases.

RESULTS AND DISCUSSION

Engineering a Potent Dominant Negative Version of Constitutively Active HSF1

Our first objective was to leverage destabilized domain (DD) technology to generate a small molecule-regulated dominant negative version of HSF1 based on extant dominant negative variants.[22,25,26] DD fusion suppresses the cellular levels of fusion proteins because the small

DD degron rapidly directs the fusion protein to the proteasome for degradation. Administration of a small molecule that stabilizes the DD prevents degradation and allows the fusion protein to function.[37–39] Transcription factors can be fused to DDs to permit small molecule-dependent, highly dosable induction of transcription factor activity.[36,40] The methodology is readily transportable, demanding minimal optimization and requiring the introduction of only a single genetic construct to bestow small molecule dose-dependent regulation of transcription factor activity.

Current dominant negative HSF1 variants typically involve deletion of a significant fraction of the C-terminal transcription activation domain of HSF1 (amino acids 379–529).[22,25,26] Our early efforts linking such dominant negative constructs to DDs indicated modest potency, suggesting that re-engineering the dominant negative HSF1 protein would be beneficial. A constitutively active version of HSF1, termed cHSF1, in which a portion of the internal regulatory domain of HSF1 (amino acids 186–202) is deleted, was previously characterized.[22,41] Induction of cHSF1 results in constitutive upregulation of HSF1-dependent genes, even in the absence of HSR activation. We rationalized that a dominant negative version of this cHSF1 variant in which the transcription activation domain (amino acids 379–529) is also deleted would prove to be a highly potent HSF1 inhibitor. Such a construct would not be subject to endogenous mechanisms for regulating HSF1 that constitutively maintain the transcription factor in its inactive, monomeric state[6] and thereby potentially reduce the potency of previously described dominant negative HSF1 variants (Figure 1A). We termed this new dominant negative version of HSF1, lacking both a portion of the internal regulatory domain and the transcription activation domain, “dn-cHSF1”.

We first assessed whether our new dn-cHSF1 construct is capable of inhibiting HSF1 by creating stable HEK293T-REx cell lines expressing dn-cHSF1 under control of the doxycycline (dox)-dependent tetracycline repressor. We predicted that induction of dn-cHSF1 would abrogate the ability of arsenite or HSP90 inhibitor-mediated activation of endogenous HSF1 to upregulate established HSR target genes. As expected, treatment of cells with arsenite or the HSP90 inhibitor STA-9090[42] results in robust induction of the HSR-regulated chaperones *HSP90 (HSP90AA1)*, *HSP70 (HSPA1A)*, and *HSP40 (DNAJB1)*. However, pre-treatment with dox for 18 h to induce dn-cHSF1 completely inhibits the arsenite- and STA-9090-mediated upregulation of these HSR genes, as observed by both RT-qPCR and Western blotting (Figures 1B,C). Thus, our new dn-cHSF1 construct is highly effective at inhibiting the HSR-mediated activation of endogenous HSF1.

dn-cHSF1 Represses HSR-Mediated Upregulation of HSF1 Target Genes With High Selectivity

We next employed whole genome transcript arrays to assess changes in the transcriptome of cells inducibly expressing dn-cHSF1 both before and after stressing with arsenite or STA-9090. Arsenite is an HSR activator that also has pleiotropic effects including oxidative stress and DNA damage. STA-9090 is a widely employed HSP90 inhibitor that rapidly activates a compensatory HSR. dn-cHSF1 provides a potential mechanism to uncouple the HSR-activating insults of arsenite or STA-9090 from the other consequences of exposure. K-Means clustering of the 3167 genes that had a significant change in mRNA levels in any

condition compared to vehicle (see Table 1 for selected genes and Table S1 for a comprehensive listing of the array data) identified a single cluster that displays significant downregulation in response to activation of dn-cHSF1 by dox treatment (Figure 2, top cluster). Gene ontology analysis revealed that this set of genes is highly enriched for HSR genes. In contrast, the large number of other genes activated by arsenite treatment (including zinc metalloproteins and genes involved in oxidative stress) are not inhibited by dn-cHSF1. Most importantly, only seven genes show a statistically significant reduction of arsenite-induced upregulation owing to dox pretreatment, all of which are classical HSR genes (shown in Table 1 in the Cytosolic Chaperones Group), highlighting the exquisite selectivity of our new dn-cHSF1 construct for HSF1 inhibition.

We next postulated that dn-cHSF1 activation provides a mechanism to uncouple the compensatory heat shock response induced by HSP90 inhibition from the direct consequences of HSP90 inhibition. To test this hypothesis, we treated cells with STA-9090 at the lowest concentration (100 nM) sufficient to inhibit HSP90, as evaluated by the resultant degradation of Akt, an established HSP90 client (Supporting Information Figure S1).[43] Treatment with 100 nM STA-9090 in our cells robustly induces the HSR, as observed by Western blotting for HSP70 and HSP40 (Supporting Information Figure S1). Unlike arsenite, which also activates multiple other cellular stress responses, our transcriptome analysis (see Table 1, Figure 2, and Supporting Information Table S1) shows that STA-9090 robustly induces (>2-fold) a set of only 18 genes, 13 of which are well-established HSR genes. Pretreatment with dox to induce dn-cHSF1 expression completely inhibits the induction of these 13 HSR genes, with no effects on the other 5 genes activated by STA-9090 treatment. The remaining five genes that remain upregulated in response to STA-9090 independent of dn-cHSF1 activation appear to be unrelated to heat shock, leading us to attribute their upregulated expression levels to pleiotropic effects of STA-9090 treatment. Thus, dn-cHSF1 induction provides a mechanism to uncouple the direct consequences of HSP90 inhibition from those effects mediated by compensatory HSR activation. This method should prove valuable in the numerous cell systems where no window exists to inhibit HSP90 (or other cytosolic chaperones) without simultaneously inducing the HSR.

Development of a Convenient and Broadly Applicable Small Molecule-Regulated Method to Inhibit Endogenous HSF1

With our highly potent and selective dn-cHSF1 construct in hand, we next anticipated that we could create a small molecule-regulated version of the dn-cHSF1 protein by fusion to an appropriate DD. To test this concept, we fused the Arg12Tyr/Tyr100Ile variant of *E. coli* DHFR, whose levels can be regulated in mammalian cells by the small molecule trimethoprim (TMP),[38] to the N-terminus of dn-cHSF1 (Figure 3A). The addition of TMP to HEK293T-REx cells expressing this DHFR.dn-cHSF1 fusion stabilizes the entire protein (Figure 3B), effectively inhibiting the HSR induced by a diverse array of stressors. For example, as shown in Figure 3C, TMP addition abrogates the HSF1-mediated transcriptional upregulation of *HSP40* induced by arsenite, the HSP90 inhibitor STA-9090, heat shock, and the HSP70 inhibitor MAL3-101.[44] These results are re-capitulated at the protein level by

immunoblotting for HSR target proteins (Figure 3D). Control experiments with DHFR.YFP-expressing cells confirm that these effects are mediated by the DHFR.dn-cHSF1 construct.

Three critical potential advantages of DD-regulation of transcription factors are: (1) high dosability, (2) rapid activation upon small molecule addition owing to the post-translational mechanism of regulation, and (3) ease of transportability into any model system of interest with minimal optimization.[36,40] Indeed, we observe that TMP addition dose-dependently suppresses HSF1 activity, allowing us to titer in distinct levels of HSF1 inhibition at will (Figure 4A). The timecourse of DHFR.dn-cHSF1 activation is also rapid. Within <2 h of TMP addition we already observe the capacity to significantly prevent arsenite-induced, HSF1-mediated induction of HSR genes, including *HSP40* (Figure 4B). Most importantly, our methodology is readily transported into various cell systems, including non-human MDCK cells (Figure 4C), with no or minimal optimization. Cumulatively, these results highlight key advantages of DD-regulation of dn-cHSF1, providing the first generally applicable method to inhibit endogenous HSF1 with high selectivity and potency in a small molecule-dependent manner in diverse cellular model systems of interest.

Orthogonal, Small Molecule-Mediated Up- and Down-Regulation of the HSR in the Absence of Stress

Acute activation of dn-cHSF1 by TMP treatment prevents HSF1 activation in response to stress. Interestingly, and consistent with previous work,[23] we find that chronic, long-term activation of DHFR.dn-cHSF1 by TMP treatment constitutively depletes cellular chaperones by inhibiting basal HSF1 activity (Figure 5A). The capacity to constitutively downregulate the cytosolic proteostasis network by DHFR.dn-cHSF1 activation, if integrated with an orthogonal method for stress-independent HSF1 activation, would allow us to create individual cell lines in which the cytosolic proteostasis network can be inducibly up- or down-regulated by treatment with orthogonal small molecules (Figure 5B). Such cell lines would be valuable for testing effects of HSF1 modulation on the proteostasis of particular normal and disease-related protein variants.

Methodology for the small molecule-mediated activation of HSF1 using the FKBP DD, which is stabilized by the small molecule Shield-1, was recently reported.[36,41] Because the DHFR and FKBP DDs are regulated by distinct small molecules, we predicted that expressing both DHFR.dn-cHSF and FKBP.cHSF1 in a single cell line would allow us to inhibit or activate HSF1 in a stress-independent manner in a single population of cells. Upon generating HEK293T-REx cells expressing both constructs, termed HEK293$^{DD.HSR}$ cells for DD-regulated control of the HSR, we observe that Shield-1 treatment robustly activates HSF1, as illustrated by the upregulation of *HSP90*, *HSP70*, and *HSP40* (Figure 5C). In contrast, TMP treatment activates DHFR.dn-cHSF1 to chronically deplete cytosolic chaperones or inhibit stress-mediated HSF1 activation. Because both FKBP.cHSF1 and DHFR.dn-cHSF1 are readily transported into any cell line of interest with minimal optimization,[36] this methodology provides a convenient mechanism to directly test the potentially contrasting effects of small molecule-mediated HSF1 activation versus small molecule-mediated HSF1 inhibition in disease model systems ranging from the protein misfolding disorders to cancer. Similar results are observed upon dox or Shield-1 treatment

in cells expressing tetracycline repressor-regulated dn-cHSF1 and FKBP.cHSF1 (which we term HEK293^{HSR} cells; Figure 5D).

Effects of HSF1 Modulation on the Behavior of Cytosolic Chaperone Clients

We next evaluated how small molecule-mediated remodeling of the cytosolic proteostasis network in HEK293^{HSR} cells influences established model cytosolic chaperone client proteins, such as firefly luciferase (FLuc).[45,46] We expected that upregulating cytosolic proteostasis mechanisms via FKBP.cHSF1 activation might enhance FLuc activity, while chronic dn-cHSF1 activation to deplete the cytosolic proteostasis network would reduce FLuc activity. Surprisingly, we observe that inhibiting endogenous HSF1 and lowering chaperone levels by inducing dn-cHSF1 significantly increases FLuc activity >2.5-fold, while Shield-1 treatment to activate HSF1 and upregulate the cytosolic proteostasis network very slightly reduces FLuc activity (Figure 6A). Interestingly, accounting for steady-state levels of cytosolic FLuc (Figure 6B) reveals that the specific activity of FLuc in basal, activated or inhibited HSF1 cellular environments is not significantly impacted by HSF1 activation or inhibition. The enhanced FLuc activity upon HSF1 inhibition cannot be attributed to globally altered protein translation, because the extent of metabolic labeling of newly synthesized proteins remains unchanged by the presence or absence of dn-cHSF1 (Figure 6C). Thus, the observed changes in FLuc activity may be attributed to modified quality control induced through chronic inhibition of endogenous HSF1, though other mechanisms could also play a role. These results highlight the complex and potentially unpredictable effects of an altered proteostasis network for some chaperone client proteins. Furthermore, the trends we observe for FLuc activity are consistent with recent work on the maladapted stress response by Balch and co-workers, who recently identified HSF1 knockdown as a potential mechanism to enhance proteostasis of misfolding globular and membrane proteins associated with genetic loss-of-function disorders.[14]

We next profiled the effects of HSF1 inhibition versus activation on the intrinsically disordered, aggregating protein polyQ$_{67}$-tdTomato,[41,45] a protein consisting of 67 glutamine residues fused to fluorescent tdTomato for visualization (Figure 6D). Polyglutamine proteins like this one are a classic example of the intrinsically disordered proteins associated with the pathology of numerous human diseases, including Huntington's disease. Various groups have speculated that modulating the proteostasis network could be a viable therapeutic strategy for such diseases.[13] Immunoblotting for polyQ$_{67}$-tdTomato from both the soluble and insoluble fractions of cell lysates suggests that the protein aggregates more aggressively in HSF1-inhibited environments (Figure 6E, note also the presence of a cleaved tdTomato band that has been previously observed for polyQ-fluorescent protein fusions and that is unaltered by modulating HSF1 activity[47]). Indeed, we find that under conditions of HSF1 inhibition the aggregation of polyQ$_{67}$-tdTomato is significantly enhanced, as determined by the appearance of fluorescent puncta identified by PULSA flow cytometry (Figures 6F and 6G and Supporting Information Figure S2 and Table S2).[48] HSF1 activation, on the other hand, does not significantly affect puncta formation, resulting in a similar amount of disperse fluorescence to untreated samples. Thus, while we find that HSF1 inhibition and consequent chaperone depletion can possibly be beneficial for soluble but poorly folding globular proteins like FLuc, these results suggest that inhibiting HSF1 and repressing the

cytosolic proteostasis network reduces the cell's capacity to handle aggregation-prone proteins.

Cumulatively, these data highlight the potentially contrasting consequences of HSF1 inhibition for different classes of misfolding proteins. For a soluble chaperone client, we observe an unexpected increase in enzyme activity upon HSF1 inhibition, an effect that could prove useful in certain protein misfolding-related diseases.[14] In contrast, HSF1 inhibition significantly enhances deleterious aggregate formation for an intrinsically disordered protein, and approaches that upregulate proteostasis network activity may prove more useful. These findings highlight the importance of considering the therapeutic relevance of both possibilities, depending on the protein misfolding-related disorder of interest, and lend credence to the concept that small molecule-mediated inhibition of HSF1 is a strategy that should be tested in cytosolic protein misfolding-related disorders.[14] Such testing should benefit greatly from our introduction of DHFR.dn-cHSF1.

CONCLUDING REMARKS

HSF1 is a high-profile target both for diseases of proteostasis and cancer. In the absence of highly selective and potent small molecule-regulated methods to inhibit HSF1 in disease model systems, understanding the beneficial and/or deleterious consequences of HSF1 inhibition remains challenging. Here, we report the development of a potent and exquisitely selective small molecule-regulated inhibitor of endogenous HSF1. Acute activation of our inhibitor abrogates the HSF1-mediated, stress-induced HSR, while chronic activation constitutively depletes cytosolic chaperones. This small molecule-regulated methodology is valuable for mechanistic experiments, where it permits the uncoupling of the direct effects of environmental toxins and chaperone inhibitors from the indirect effects of the compensatory HSR induced by these compounds. Furthermore, integration of our method with a previously reported small molecule-based technique to activate HSF1[36] permits the generation of enhanced or repressed cytosolic proteostasis networks using orthogonal, stress-independent small molecules in a single population of cells. Intriguingly, we find that the consequences of HSF1 inhibition versus activation on proteostasis are not always intuitive. For a model, chaperone-dependent soluble protein, HSF1 inhibition has the beneficial effect of significantly increasing enzyme activity, while HSF1 activation very modestly reduces enzyme activity. In contrast, for the alternative case of an intrinsically disordered, aggregation-prone protein, HSF1 inhibition enhances deleterious protein aggregation. These results highlight the value of selective and potent chemical biology methods to inhibit HSF1, allowing hypothesis testing in disease-relevant systems to guide rational therapeutic development efforts and elucidation of the critical roles of HSF1 in tumorigenesis and cancer progression.

METHODS

Reagents, Plasmids, and Antibodies

Sodium arsenite 0.1 N standardized solution was purchased from Alfa Aesar, STA-9090 was purchased from MedChem Express, MAL3-101 was purchased from ChemTech, Inc., and Shield-1 was purchased from ClonTech. FLuc-GFP.pCIneo was a generous gift from Prof.

F.-U. Hartl (Max Planck Institute).[45] pTDtomato-N1-Q0-TDtomato and pTDtomato-N1-polyQ67-TDtomato plasmids were a generous gift from Prof. R. Morimoto (Northwestern).[41] To construct dn-cHSF1.pENTR1A and DHFR.dn-cHSF1.pENTR1A, the DNA fragment corresponding to dn-cHSF1 was PCR-amplified using DNA oligonucleotides aaaaaaggtaccaccatggatctgcccgtggg and aaaaaagcggccgcctacaggcaggctacgctga as primers and cHSF1.pENTR1A as the template.[36] The PCR product was digested with KpnI and NotI, and then cloned into KpnI- and NotI-digested pENTR1A (Life Technologies) or DHFR.YFP.pENTR1A vectors.[38] Genes of interest in pENTR1A were shuttled into appropriate destination vectors using LR clonase II-mediated recombination (Life Technologies). The following antibodies were used: mouse monoclonal anti-β-actin from rabbit polyclonal anti-HSF1 from Sigma, anti-HSP70/72 and anti-HSP40/Hdj1 from Enzo Life Sciences, rabbit monoclonal anti-HSP90 from Cell Signaling, and rabbit polyclonal anti-GFP from GeneTex.

Cell Culture

HEK293T-REx (Life Technologies) and MDCK cells and were cultured at 37 °C in a 5% CO_2 atmosphere in DMEM (CellGro) supplemented with 10% fetal bovine serum (CellGro) and 1% penicillin/streptomycin/glutamine (CellGro). Lentiviruses encoding dox-inducible dn-cHSF1 and DHFR.dn-cHSF1 prepared as described in the Supporting Information were transduced into either MDCK cells, HEK293T-REx cells, or previously described HEK293T-REx cells already stably expressing FKBP.cHSF1.[36] Stable cell lines were selected by culturing in complete medium containing G418, blasticidin, Zeocin, hygromycin and/or puromicyin, as appropriate, prior to single-colony selection and characterization. Transient transfections of polyglutamine and FLuc-GFP.pCIneo constructs were performed using polyethylenimine.

Immunoblotting

Proteins were separated by SDS-PAGE and then transferred to nitrocellulose membr anes. Following blocking and incubation with appropriate primary antibodies, membranes were incubated with 680 or 800 nm fluorophore-labeled secondary antibodies (Li-COR Biosciences) prior to detection using a LI-C OR Biosciences Odyssey Imager. Band intensity quantification was performed in Image Studio Lite (LI-COR Biosciences).

Quantitative RT-PCR

The relative mRNA expression levels of target genes were measured using the detailed protocol presented in the Supporting Information; primers used are listed in Supporting Information Table S3.

Whole Genome Microarrays

HEK293T-REx cells expressing dox-inducible dn-cHSF1 were treated for 18 h with vehicle or 1 μg/mL dox prior to HSF1 activation by treatment with arsenite (100 μM for 4 h) or STA-9090 (10 nM for 8 h), all in biological triplicate. Cells were harvested, and RNA was extracted using the RNeasy Plus Mini Kit (Qiagen). RNA quality was confirmed using a Fragment Analyzer (Advanced Analytical). RNA samples were labeled for hybridization

using NuGEN ovation kit and hybridized to Affymetrix human Primeview microarrays. Mircoarray data were extracted using Affymetrix Expression Console and analyzed using the Affymetrix Transciptome Analysis Console 3.0.

Luciferase Activity Assays

After pretreatment with the appropriate small molecule and/or stressor, cells were lysed by adding luciferase lysis buffer (Promega) directly to the wells and incubated in the dark at rt for 15 min. Following a 5 min spin to remove insoluble cell debris, 50 μL lysate was added to a white, opaque 96-well plate with 50 μL of the Bright-Glo Luciferase Assay System buffer (Promega). Following a 15 s double-orbital mix cycle, luminescence was recorded on a BioTek Synergy H1 Hybrid Reader. Measurement times using luminescence fiber were set to 0.4 sec integration time per well. A four-point mean maximum calculation was used to determine the luminescence. To determine specific activities, the luminescence values (FLuc activities) were divided by FLuc band intensity quantified from immunoblots by densitometry using the LI-COR Image Studio Lite software.

[^{35}S] Metabolic Labeling Experiments

HEK293^{HSR} cells transiently transfected with FLuc were seeded on poly-D-lysine-coated plates and treated with vehicle, dox at 1 μg/mL to activate dn-cHSF1, or Shield-1 at 1 μM to activate cHSF1 for 48 h. Cells were then starved for 30 min in DMEM + 10% FBS lacking Cys and Met. Cells were metabolically labeled in pulse medium containing [^{35}S]-Cys/Met (MP Biomedical, ~0.1 mCi/mL final concentration) for 15 min prior to lysis. Cells were lysed in a 1% Triton X-100 buffer. Lysates were boiled in 1X-Laemmli buffer and separated by SDS-PAGE. The gels were then dried, exposed to phosphorimager plates (GE Healthcare), and imaged with a Typhoon imager.

Flow Cytometry

Cells were analyzed at a slow flow rate in an LSRFortessa flow cytometer (BD Biosciences). 10,000 events were collected per measurement, using a forward scatter threshold of 5,000 and obtaining pulse height, area and width parameters for each channel. For dTomato, data were collected with the 561-nm laser and 610/20 nm bandpass filter. Flow cytometry data were analyzed using FACSDiva software (BD Biosciences).

Supplementary Material

Refer to Web version on PubMed Central for supplementary material.

Acknowledgments

This work was supported by the Mallinckrodt Foundation Faculty Scholar Award, the Smith Family Foundation Excellence in Biomedical Research Award, the Office of the Director of the US National Institutes of Health (NIH Grant 1DP2GM119162), the MIT Center for Environmental Health Sciences (NIH Grant P30-ES002109), MIT, and the MIT Department of Chemistry (all to M.D.S.). C.L.M. was supported by an NSF Graduate Research Fellowship. E.E.N. was supported by a UNCF-Merck Postdoctoral Fellowship.

References

1. Åkerfelt M, Morimoto RI, Sistonen L. Heat shock factors: integrators of cell stress, development and lifespan. Nat Rev Mol Cell Biol. 2010; 11:545–555. [PubMed: 20628411]
2. Anckar J, Sistonen L. Regulation of HSF1 function in the heat stress response: implications in aging and disease. Annu Rev Biochem. 2011; 80:1089–1115. [PubMed: 21417720]
3. Trinklein ND, Murray JI, Hartman SJ, Botstein D, Myers RM. The role of heat shock transcription factor 1 in the genome-wide regulation of the mammalian heat shock response. Mol Biol Cell. 2004; 15:1254–1261. [PubMed: 14668476]
4. Zuo JR, Baler R, Dahl G, Voellmy R. Activation of the DNA-binding ability of human heat-shock transcription factor-1 may involve the transition from an intramolecular to an intermolecular triple-stranded coiled-coil structure. Mol Cell Biol. 1994; 14:7557–7568. [PubMed: 7935471]
5. Zou JY, Guo YL, Guettouche T, Smith DF, Voellmy R. Repression of heat shock transcription factor HSF1 activation by HSP90 (HSP90 complex) that forms a stress-sensitive complex with HSF1. Cell. 1998; 94:471–480. [PubMed: 9727490]
6. Voellmy R. On mechanisms that control heat shock transcription factor activity in metazoan cells. Cell Stress Chaper. 2004; 9:122–133.
7. Whitesell L, Lindquist S. Inhibiting the transcription factor HSF1 as an anticancer strategy. Expert Opin Ther Tar. 2009; 13:469–478.
8. Dai C, Whitesell L, Rogers AB, Lindquist S. Heat shock factor 1 is a powerful multifaceted modifier of carcinogenesis. Cell. 2007; 130:1005–1018. [PubMed: 17889646]
9. Santagata S, Hu R, Lin NU, Mendillo ML, Collins LC, Hankinson SE, Schnitt SJ, Whitesell L, Tamimi RM, Lindquist S, Ince TA. High levels of nuclear heat-shock factor 1 (HSF1) are associated with poor prognosis in breast cancer. Proc Natl Acad Sci USA. 2011; 108:18378–18383. [PubMed: 22042860]
10. Scherz-Shouval R, Santagata S, Mendillo ML, Sholl LM, Ben-Aharon I, Beck AH, Dias-Santagata D, Koeva M, Stemmer SM, Whitesell L, Lindquist S. The reprogramming of tumor stroma by HSF1 is a potent enabler of malignancy. Cell. 2014; 158:564–578. [PubMed: 25083868]
11. Mendillo ML, Santagata SKM, Bell GW, Hu R, Tamimi RM, Fraenkel E, Ince TA, Whitesell L, Lindquist S. HSF1 drives a transcriptional program distinct from heat shock to support highly malignant human cancers. Cell. 2012; 150:549–562. [PubMed: 22863008]
12. Chen YY, Chen JY, Loo A, Jaeger S, Bagdasarian L, Yu JJ, Chung F, Korn J, Ruddy D, Guo RB, Mclaughlin ME, Feng F, Zhu P, Stegmeier F, Pagliarini R, Porter D, Zhou WL. Targeting HSF1 sensitizes cancer cells to HSP90 inhibition. Oncotarget. 2013; 4:816–829. [PubMed: 23615731]
13. Balch WE, Morimoto RI, Dillin A, Kelly JW. Adapting proteostasis for disease intervention. Science. 2008; 319:916–919. [PubMed: 18276881]
14. Roth DM, Hutt DM, Tong JS, Bouchecareilh M, Wang N, Seeley T, Dekkers JF, Beekman JM, Garza D, Drew L, Masliah E, Morimoto RI, Balch WE. Modulation of the maladaptive stress response to manage diseases of protein folding. PLoS Biol. 2014; 12:e10011998.
15. Au QY, Zhang YJ, Barber JR, Ng SC, Zhang B. Identification of inhibitors of HSF1 functional activity by high-content target-based screening. J Biomol Screen. 2009; 14:1165–1175. [PubMed: 19820069]
16. Kim JA, Kim Y, Kwon BM, Han DC. The natural compound Cantharidin induces cancer cell death through inhibition of heat shock protein 70 (HSP70) and Bcl-2-associated athanogene domain 3 (BAG3) expression by blocking heat shock factor 1 (HSF1) binding to promoters. J Biol Chem. 2013; 288:28713–28726. [PubMed: 23983126]
17. Westerheide SD, Kawahara TLA, Orton K, Morimoto RI. Triptolide, an inhibitor of the human heat shock response that enhances stress-induced cell death. J Biol Chem. 2006; 281:9616–9622. [PubMed: 16469748]
18. Santagata S, Mendillo ML, Tang YC, Subramanian A, Perley CC, Roche SP, Wong B, Narayan R, Kwon H, Koeva M, Amon A, Golub TR, Porco JA Jr, Whitesell L, Lindquist S. Tight coordination of protein translation and HSF1 activation supports the anabolic malignant state. Science. 2013; 341:1238303. [PubMed: 23869022]

19. Schilling D, Kuhnel A, Tetzlaff F, Konrad S, Multhoff G. NZ28-induced inhibition of HSF1, SP1 and NF-kappaB triggers the loss of the natural killer cell-activating ligands MICA/B on human tumor cells. Cancer Immunol Immunother. 2015; 64:599–608. [PubMed: 25854583]
20. Smurnyy Y, Cai M, Wu H, McWhinnie E, Tallarico JA, Yang Y, Feng Y. DNA sequencing and CRISPR-Cas9 gene editing for target validation in mammalian cells. Nat Chem Biol. 2014; 10:623–625. [PubMed: 24929529]
21. Xia WL, Vilaboa N, Martin JL, Mestril R, Guo YL, Voellmy R. Modulation of tolerance by mutant heat shock transcription factors. Cell Stress Chaper. 1999; 4:8–18.
22. Voellmy R. Dominant-positive and dominant-negative heat shock factors. Methods. 2005; 35:199–207. [PubMed: 15649847]
23. Heldens L, Dirks RP, Hensen SMM, Onnekink C, van Genesen ST, Rustenburg F, Lubsen NH. Co-chaperones are limiting in a depleted chaperone network. Cell Mol Life Sci. 2010; 67:4035–4048. [PubMed: 20556630]
24. Heldens L, van Genesen ST, Hanssen LLP, Hageman J, Kampinga HH, Lubsen NH. Protein refolding in peroxisomes is dependent upon an HSF1-regulated function. Cell Stress Chaper. 2012; 17:603–613.
25. Wang JH, Yao MZ, Gu JF, Sun LY, Shen YF, Liu XY. Blocking HSF1 by dominant-negative mutant to sensitize tumor cells to hyperthermia. Biochem Biophys Res Commun. 2002; 290:1454–1461. [PubMed: 11820785]
26. Wang Y, Theriault JR, He H, Gong J, Calderwood SK. Expression of a dominant negative heat shock factor-1 construct inhibits aneuploidy in prostate carcinoma cells. J Biol Chem. 2004; 279:32651–32659. [PubMed: 15152009]
27. Verma P, Pfister JA, Mallick S, D'Mello SR. HSF1 protects neurons through a novel trimerization- and HSP-independent mechanism. J Neurosci. 2014; 34:1599–15612. [PubMed: 24478344]
28. Evans CG, Chang L, Gestwicki JE. Heat shock protein 70 (Hsp70) as an emerging drug target. J Med Chem. 2010; 53:4585–4602. [PubMed: 20334364]
29. Whitesell L, Lindquist SL. HSP90 and the chaperoning of cancer. Nat Rev Canc. 2005; 5:761–772.
30. Baldo B, Weiss A, Parker CN, Bibel M, Paganetti P, Kaupmann K. A screen for enhancers of clearance identifies Huntingtin as a heat shock protein 90 (Hsp90) client protein. J Biol Chem. 2012; 287:1406–1414. [PubMed: 22123826]
31. Wang Y, McAlpine SR. Combining an Hsp70 inhibitor with either an N- or C-terminal Hsp90 inhibitor produces mechanistically distinct phenotypes. Org Biomol Chem. 2015; 13:3691–3698. [PubMed: 25679754]
32. Burlison JA, Neckers L, Smith AB, Maxwell A, Blagg BSJ. Novobiocin: Redesigning a DNA gyrase inhibitor for selective inhibition of Hsp90. J Am Chem Soc. 2006; 128:15529–15536. [PubMed: 17132020]
33. Koay YC, McConnell JR, Wang Y, Kim SJ, Buckton LK, Mansour F, McAlpine SR. Chemically accessible HSP90 inhibitor that does not induce a heat shock response. ACS Med Chem Lett. 2014; 5:771–776. [PubMed: 25050163]
34. Garg G, Zhao HP, Blagg BSJ. Design, synthesis, and biological evaluation of ring-constrained Novobiocin analogues as Hsp90 C-terminal inhibitors. ACS Med Chem Lett. 2015; 6:204–209. [PubMed: 25699150]
35. Del Razo LM, Quintanilla-Vega B, Brambila-Colombres E, Calderon-Aranda ES, Manno M, Albores A. Stress proteins induced by arsenic. Toxicol Appl Pharm. 2001; 177:132–148.
36. Shoulders MD, Ryno LM, Cooley CB, Kelly JW, Wiseman RL. Broadly applicable methodology for the rapid and dosable small molecule-mediated regulation of transcription factors in human cells. J Am Chem Soc. 2013; 135:8129–8132. [PubMed: 23682758]
37. Banaszynski LA, Chen LC, Maynard-Smith LA, Ooi AGL, Wandless TJ. A rapid, reversible, and tunable method to regulate protein function in living cells using synthetic small molecules. Cell. 2006; 126:995–1004. [PubMed: 16959577]
38. Iwamoto M, Björklund T, Lundberg C, Kirik D, Wandless TJ. A general chemical method to regulate protein stability in the mammalian central nervous system. Chem Biol. 2010; 17:981–988. [PubMed: 20851347]

39. Miyazaki Y, Imoto H, Chen LC, Wandless TJ. Destabilizing domains derived from the human estrogen receptor. J Am Chem Soc. 2012; 134:3942–3945. [PubMed: 22332638]
40. Shoulders MD, Ryno LM, Genereux JC, Moresco J, Tu PG, Wu CL, Yates JRI, Su AI, Kelly JW, Wiseman RL. Stress-independent activation of XBP1s and/or ATF6 reveals three functionally diverse ER proteostasis environments. Cell Rep. 2013; 3:1279–1292. [PubMed: 23583182]
41. Ryno LM, Genereux JC, Naito T, Morimoto RI, Powers ET, Shoulders MD, Wiseman RL. Characterizing the altered cellular proteome induced by the stress-independent activation of heat shock factor I. ACS Chem Biol. 2014:1273–12783. [PubMed: 24689980]
42. Ying WW, Du ZJ, Sun LJ, Foley KP, Proia DA, Blackman RK, Zhou D, Inoue T, Tatsuta N, Sang J, Ye SX, Acquaviva J, Ogawa LS, Wada Y, Barsoum J, Koya K. Ganetespib, a unique triazolone-containing HSP90 inhibitor, exhibits potent antitumor activity and a superior safety profile for cancer therapy. Mol Cancer Ther. 2012; 11:475–484. [PubMed: 22144665]
43. Sato S, Fujita N, Tsuruo T. Modulation of Akt kinase activity by binding to Hsp90. Proc Natl Acad Sci USA. 2000; 97:10832–10837. [PubMed: 10995457]
44. Fewell SW, Smith CM, Lyon MA, Dumitrescu TP, Wipf P, Day BW, Brodsky JL. Small molecule modulators of endogenous and co-chaperone-stimulated Hsp70 ATPase activity. J Biol Chem. 2004; 279:51131–51140. [PubMed: 15448148]
45. Gupta R, Kasturi P, Bracher A, Loew C, Zheng M, Villella A, Garza D, Hartl FU, Raychaudhuri S. Firefly luciferase mutants as sensors of proteome stress. Nat Methods. 2011; 8:879–886. [PubMed: 21892152]
46. Schumacher RJ, Hurst R, Sullivan WP, McMahon NJ, Toft DO, Matts RL. ATP-dependent chaperoning activity of reticulocyte lysate. J Biol Chem. 1994; 269:9493–9499. [PubMed: 8144534]
47. Holmberg CI, Staniszewski KE, Mensah KN, Matouschek A, Morimoto RI. Inefficient degradation of truncated polyglutamine proteins by the proteasome. EMBO J. 2004; 23:4307–4318. [PubMed: 15470501]
48. Ramdzan YM, Polling S, Chia CPZ, Ng IHW, Ormsby AR, Croft NP, Purcell AW, Bogoyevitch MA, Ng DCH, Gleeson PA, Hatters DM. Tracking protein aggregation and mislocalization in cells with flow cytometry. Nat Methods. 2012; 9:467–476. [PubMed: 22426490]

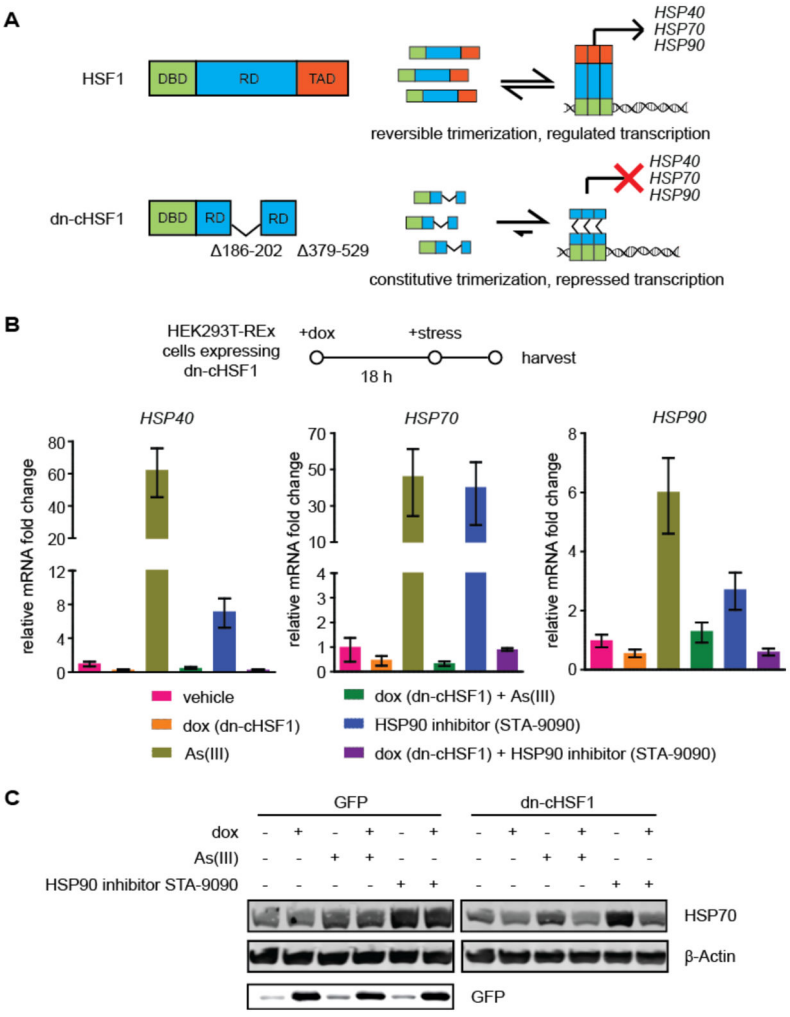

Figure 1. Design and validation of a new, potent dominant negative HSF1 variant "dn-cHSF1"

(A) Models of cHSF1 and dn-cHSF1, which lacks a portion of the internal regulatory domain (RD; deleted amino acids 186–202) and the C-terminal transcription activation domain (amino acids 379–529).

(B) qPCR analysis of *HSP40 (DNAJB1)*, *HSP70 (HSPA1A)*, and *HSP90* (*HSP90AA1*) in HEK293T-REx cells inducibly expressing dn-cHSF1 following pretreatment with vehicle or dox (18 h; 1 μg/mL) and then HSR activation by treatment with arsenite (6 h; 100 μM) or STA-9090 (6 h; 100 nM). qPCR data are reported as the mean ±95% confidence interval relative to vehicle-treated HEK293T-REx cells.

(C) Immunoblot of cells in Figure 1B showing inhibition of HSR activation by induction of dn-cHSF1.

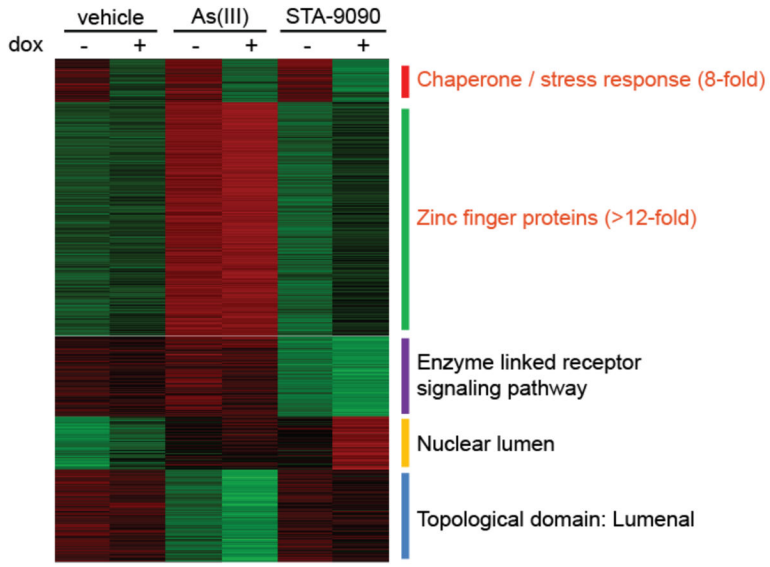

Figure 2. Transcriptional profiling of the selective inhibition of HSF1 upon dn-cHSF1 activation

A five-node K-means clustergram performed on genes showing an experiment-wide ANOVA of <0.001 in array data obtained from HEK293-TREx cells inducibly expressing dn-cHSF1 following pretreatment with vehicle or dox (18 h; 1 μg/mL) and then subjected to HSR activation by treatment with arsenite (6 h; 100 μM) or STA-9090 (6 h; 100 nM). Red corresponds to high relative transcript levels and green corresponds to low relative transcript levels. Listed next to each node is the strongest gene ontology (GO) assignment based on enrichment scores from DAVID GO analysis of gene sets. Labels in red correspond to GO assignments with an enrichment score >2 fold over expected.

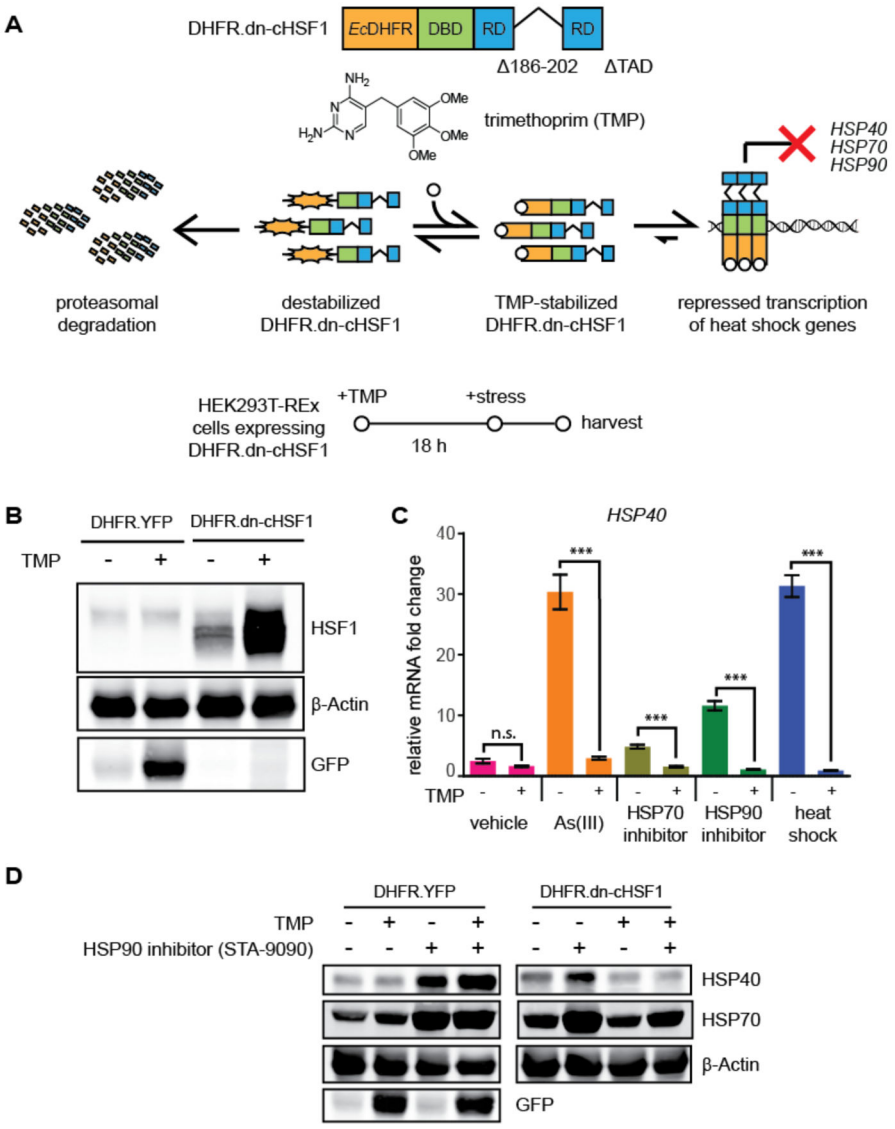

Figure 3. Application of destabilized domains to inhibit HSF1 in a small molecule-dependent manner

(A) Model showing the TMP-dependent regulation of the DHFR.dn-cHSF1 fusion protein. The structure of TMP is shown.

(B) Immunoblot of HEK293T-REx cells expressing DHFR.YFP or DHFR.dn-cHSF1. TMP (10 μM) was added 18 h prior to harvest.

(C) qPCR analysis of *HSP40* in HEK293T-REx cells expressing DHFR.dn-cHSF1. Vehicle (DMSO) or TMP (10 μM) was added for 12 h, followed by treatment with arsenite (100 μM; 6 h), HSP90 inhibitor STA-9090 (100 nM; 6 h), HSP70 inhibitor MAL3-101 (10 nM; 6 h) or heat shock (42 °C; 2 h). qPCR data are presented as fold-increase relative to vehicle-treated cells expressing DHFR.YFP. Error bars represent SEM from biological replicates (n = 3). ***$p < 0.0001$.

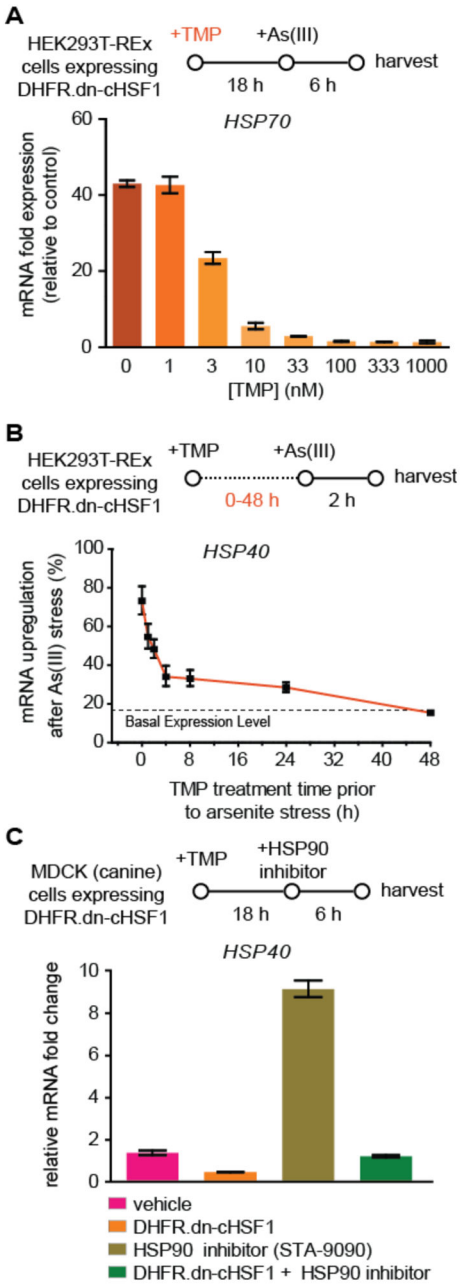

Figure 4. Advantages of small molecule-mediated inhibition of HSF1 with DHFR.dn-cHSF1

(A) qPCR analysis of *HSP40* in HEK293T-REx cells expressing DHFR.dn-cHSF1 pretreated with increasing concentrations of TMP for 18 h prior to HSR activation by arsenite treatment (100 μM; 6 h).

(B) qPCR analysis of *HSP40* in HEK293T-REx cells expressing DHFR.dn-cHSF1 pretreated with TMP (10 μM) for the indicated times prior to HSR activation by arsenite treatment (100 μM; 2 h). The expression of *HSP40* was normalized to the maximal expression observed upon arsenite treatment with no TMP pretreatment.

(C) qPCR analysis of HSF1 target genes in MDCK cells expressing DHFR.dn-cHSF1, pretreated with TMP (10 μM; 18 h) and then treated with arsenite (100 μM; 6 h) to activate the HSR.

All qPCR data are presented as the mean ±95% confidence interval relative to vehicle-treated cells.

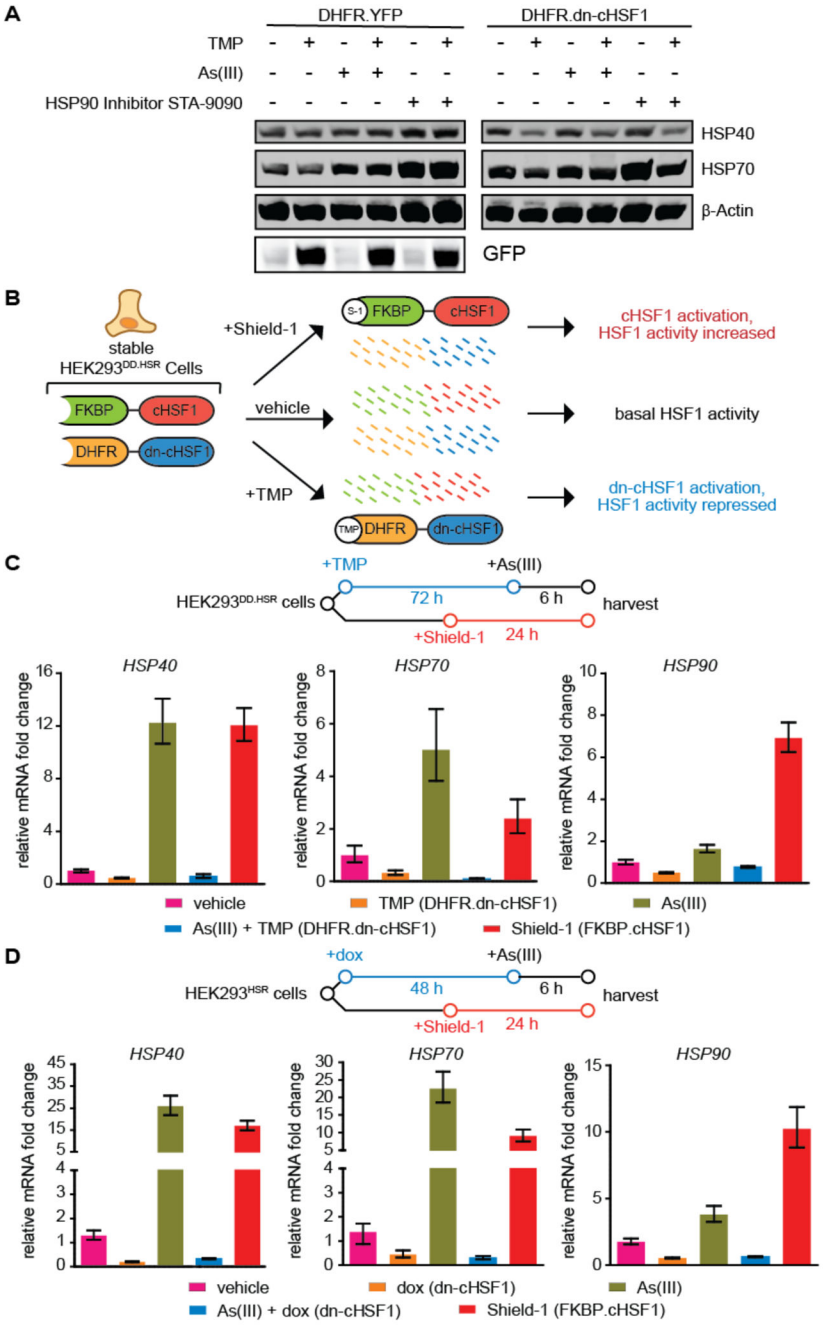

Figure 5. Inhibition and activation of HSF1 with orthogonal small molecules in a single population of HEK293 cells

(A) Immunoblot showing the depletion of cellular chaperones upon chronic activation of DHFR.dn-cHSF1 by treatment with TMP (10 μM; 72 h).

(B) Illustration showing the incorporation of both DHFR.dn-cHSF1 and FKBP.cHSF1 into a single cell line.

(C) qPCR analysis of HSF1 target genes in HEK293$^{DD.HSR}$ cells expressing both TMP-regulated DHFR.dn-cHSF1 and FKBP.cHSF1. Cells were treated with TMP (10 μM; 78 h),

Shield-1 (1 μM; 24 h), arsenite (100 μM; 6 h), or pre-treated with TMP (10 μM; 72 h) followed by arsenite (100 μM; 6 h).

(D) qPCR analysis of HSF1 target genes in HEK293^{HSR} cells expressing both dox-regulated dn-cHSF1 and FKBP.cHSF1. Cells were treated with dox (1 μg/mL; 54 h), Shield-1 (1 μM; 24 h), arsenite (100 μM; 6 h), or pre-treated with dox (1 μg/mL; 48 h) followed by arsenite (100 μM; 6 h).

All qPCR data are reported as the mean ±95% confidence interval relative to vehicle-treated HEK293T-REx cells.

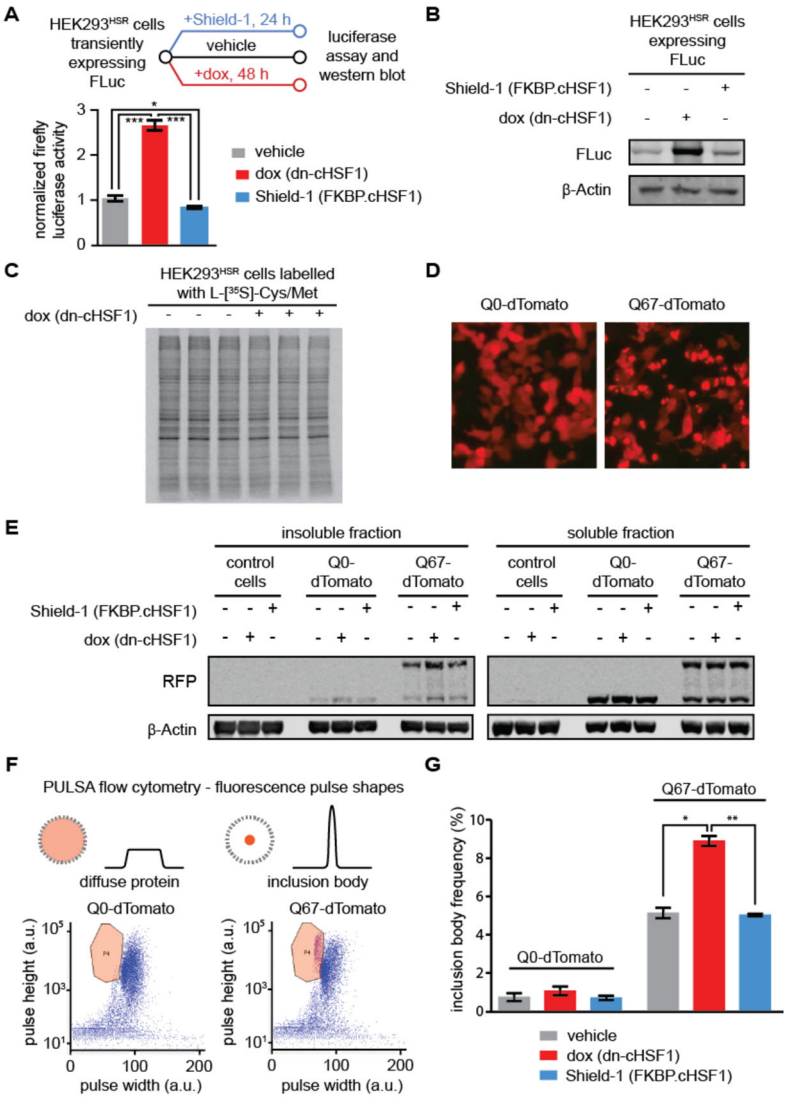

Figure 6. Effects of HSF1 inhibition and activation on the folding of a globular cytosolic chaperone client

(A) Experimental workflow showing FLuc activity measured in transiently transfected HEK293T-REx^{HSR} cells after treatment with vehicle, dox to induce HSF1 inhibition (1 μg/mL; 48 h), or Shield-1 to activate cHSF1 (1 μM; 48 h). Error bars represent SEM from biological replicates (n = 3). Significance was calculated using the paired Student's two-tailed *T*-test. *$p < 0.05$, ***$p < 0.005$.

(B) Immunoblot to assay steady-state levels of FLuc after the treatments used in Figure 6A. (C) Auto-radiogram of [^{35}S]-labelled protein from HEK293^{HSR} lysates expressing dn-cHSF1 (dox; 1 μg/mL, 48 h) or no treatment prior to 15 min metabolic labelling with L-[^{35}S]-methionine.

(D) Epifluorescent microscopy images of HEK293^{HSR} cells transiently transfected with plasmids encoding Q_0-tdTomato (left) or polyQ_{67}-tdTomato (right)) and then treated with vehicle, dox to induce HSF1 inhibition (1 μg/mL; 48 h), or Shield-1 to activate cHSF1 (1 μM; 48 h).

(E) Immunoblot of soluble and insoluble fractions from HEK293^{HSR} cells in Figure 6D. **(F)** Diagram of PULSA flow cytometry, which utilizes fluorescence pulse height and pulse width information to identify inclusion bodies in live cells. Shown are representative plots of HEK293^{HSR} cell populations transiently transfected with Q_0-tdTomato (left) and polyQ_{67}-tdTomato (right) treated as in Figure 6D, with gating for inclusion body population defined as the region bounded by the orange line. Purple dots in this region are defined as live cells with inclusion bodies, while all other events on the plot are defined as live cells. **(G)** Quantification of inclusion body frequency measured by PULSA flow cytometry analysis of HEK293^{HSR} cells in Figure 6E. Error bars represent SEM from 10,000 recorded live cell events performed on biological replicates (n = 3). *$p < 0.05$, **$p < 0.01$.

Table 1

Analysis of dn-cHSF1-mediated heat shock response inhibition specificity (see also Table S1).

RNA Array Fold Change Relative to Vehicle-Treated Cells[a]				
Gene	**Arsenite**	**Arsenite + dn-cHSF1**	**HSP90 Inhibitor**	**HSP90 Inhibitor + dn-cHSF1**
Cytosolic Chaperones				
HSPA1A; HSPA1B	**13.15**	0.52	**18.68**	1.19
HSPA6; HSPA7	**18.04**	0.66	**8.47**	0.62
HSPA6	**13.88**	0.85	**7.04**	0.72
DNAJB1	**3.43**	0.38	**3.31**	0.38
HSPH1	**2.28**	1.29	**2.92**	0.95
DNAJA1	**1.76**	0.94	**1.82**	0.9
HSP90AA1	**1.39**	0.66	**1.78**	0.69
Oxidative Stress Genes				
HMOX1	**27.67**	**16.92**	1.15	0.8
CTH	**8.47**	**8.37**	1.3	3.47
MT1X	**25.55**	**24.8**	1.16	1.33
MT1F	**16.2**	**19.01**	1.13	1.44
Zinc Metalloproteins and Transporters				
ZNF195	**2.09**	**2.29**	1.22	1.34
ZNF33A	**1.4**	**1.33**	1.12	1.01
ZFP69B	**5.65**	**6.93**	1.09	1.8
ZNF10	**2.19**	**2.13**	1.07	1.16
SLC30A1	**3.37**	**4.05**	1.06	0.97
ZMYM3	**0.45**	**0.43**	1.06	0.85
DPF2	**1.51**	**1.52**	0.98	0.98
SLC30A2	**6.00**	**12.89**	0.96	1.3
SLC30A1	**4.34**	**4.92**	0.92	0.98
ZNF674	**2.33**	**2.21**	0.73	1.07
Endoplasmic Reticulum Chaperones				
HSPA5 (GRP78/BIP)	0.81	0.83	0.77	0.96
GRP94	0.88	0.84	0.98	1.01
DNAJB11 (ERDJ3)	0.81	0.89	0.85	0.81
DNAJB9 (ERDJ4)	1.06	0.99	1.00	1.22
DNAJC10 (ERDJ5)	1.01	0.80	0.99	0.93
HYOU1	1.04	0.98	1.13	1.05
Disulfide Redox				
PDIA3	1.15	1.00	1.01	1.08

RNA Array Fold Change Relative to Vehicle-Treated Cells[a]				
Gene	**Arsenite**	**Arsenite + dn-cHSF1**	**HSP90 Inhibitor**	**HSP90 Inhibitor + dn-cHSF1**
PDIA4	1.04	1.00	1.15	1.17
PDIA6	0.85	0.75	0.90	0.99
ERO1L	0.93	0.83	0.97	1.02
ERO1LB	1.11	1.24	0.73	1.03

[a]Bolded text indicates an ANOVA p-value <0.001 relative to vehicle-treated cells. All un-bolded text indicates no significant change with respect to vehicle-treated cells.